



In Vitro and *In Vivo* Effectiveness of GPK/B20, A Phytocomplex in Two Experimental Flu Virus Models

Rastmanesh R¹, Kushugulova A², Kumar N³, Nagyzbekkyzy E², Rasulova S⁴, Lorenzetti A⁴ and He F^{5*}

¹Nutrition Researcher, member of Nutrition Society of London, UK

²Center for Life Sciences, NLA, Nazarbayev University, National Laboratory Astana, Republic of Kazakhstan

³Faculty of Applied Sciences, Shri Venkateshwara University, JP Nagar, Uttar Pradesh, India

⁴ReGenera R&D International for Aging Intervention, Italy

⁵Department of Nutrition, Food Safety and Toxicology, West China School of Public Health, Sichuan University, China

***Corresponding author:** He Fang, Department of Nutrition, Food Safety and Toxicology, West China School of Public Health, Sichuan University, Chengdu, China, Email: nrb47389@nifty.com

Research Article

Volume 5 Issue 1

Received Date: January 28, 2021

Published Date: March 05, 2021

DOI: 10.23880/oajpr-16000228

Abstract

There is constant quest to prevent and counterfight annual influenza viral epidemics, given the limitations and drawbacks of antiviral chemicals so far. The aim of the present study was to test on an experimental viral model a phytocompound containing herbal ingredients endowed by, albeit scattered, reports of antiviral properties (GPK/B20, Viraxil, Named, Italy). Two influenza models were employed, i.e. H1N1 and H3N2. In vitro test showed that GSK/B20, especially at medium and high dose (50µl/mL to 100µl/mL) significantly reduced the infection of Madin-Darby-Canine-Kidney monolayers cells and progression of cytopathogenic effect over the observation period. More interestingly, when this compound was test 1h after infection on mice, especially at high dose (60g/kg/day), it appeared to significantly blunt the immune/inflammatory cells recruitment and the inflammatory cytokine cascade (at lung tissue level and bronco-alveolar lavage level), curbing also the related gene expression. This was associated to a reduced lung oedema, which is the correlate of respiratory distress in humans, viral load and scanning electron microscopy findings. In the meantime, more detailed experimental studies are warranted to unveil the range of mechanisms of actions that these natural ingredients are likely to be endowed with. Although these data have to be taken with caution having being obtained in an experimental-controlled setting, they suggest a potential safe application in the clinical practice, as recently corroborated for one of the herbal used.

Keywords: Flu Model; GPK/B20; H1N1; H3N2; Antiviral Effect

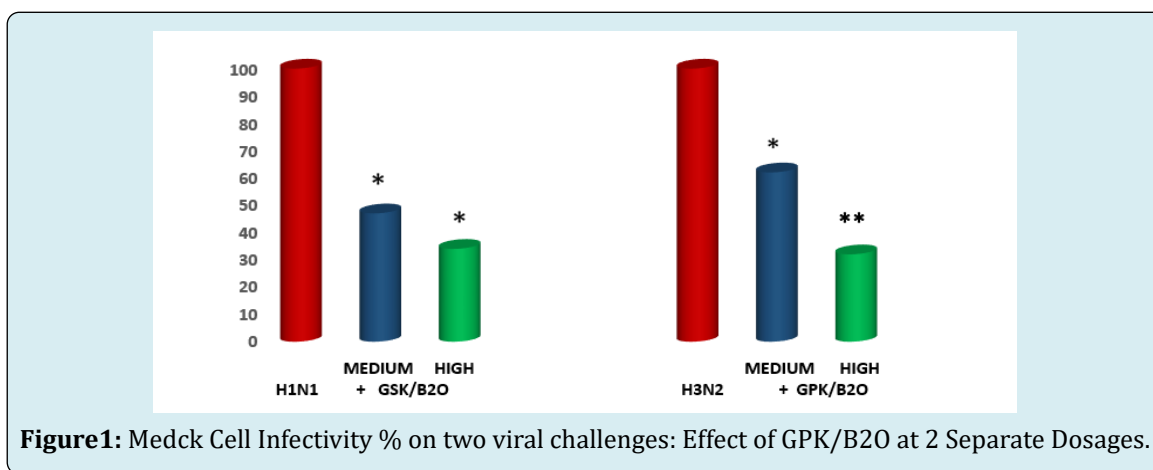
Introduction

Influenza viruses are classified as type A, B, C and D on the basis of their the viral nucleoprotein and major matrix protein antigenic characteristics. As a matter of fact only influenza A and B viruses are reported to be the largely predominant cause of human disease. The influenza virus is,

by far, the most frequently encountered respiratory illness widely spreading worldwide. Between 25 to 50 million individuals are affected every year and causing close to 200,000 hospitalization in USA and leading to 250,000 to 500,000 deaths worldwide every year. As average, the death toll in USA is in excess of 35,000 cases with pandemics peaks, as in recent times with multiplied figures [1]. Generally

speaking, the IFV are usually ascribed to strains belonging to a well defined group, such as para influenza viruses, influenza, rhinoviruses, corona viruses, respiratory syncytial virus, and some adenoviruses. The vaccine countermeasures deployed each year are specifically targeted to a strain and updated on a year basis. This is because the viral RNA structure is liable to undergo a great deal as genetic or antigenic “drift” mutations and re-assembling with a number of viral sub-types of human or animal origin, at times generating even more detrimental “shift” [2]. Moreover, the spectrum of viral respiratory syndromes is embracing a wide scenario consisting of influenza virus A or B, influenza-like

illness and common cold. The first has a seasonal, highly contagious and a recurrent epidemic/pandemic nature whereas the latter being mostly a self-limiting acute viral rhinopharyngitis caused by rhinoviruses and corona viruses. With the above-mentioned limitations, from the treatment viewpoint, the three main classes of drugs belong to matrix protein, ion channel inhibitors, such as amantadine and rimantadine, neuraminidase inhibitors such as oseltamivir, zanamivir, laninamivir and peramivir and anti-viral RNA polymerase effectors, namely ribavirin and favipiravir. The main drawback of these drugs is their tendency to generate virus resistance [3].



The past lesson with these drug approach has indeed taught that it is very likely that most novel similar drugs in the current pharma pipeline stand high chance to eventually trigger and inner viral resistance via the occurrence of mutants variability [4]. However, such pharmacological approaches lack specificity and normally promote a delayed response or yield a modest efficacy, Systemic corticosteroids are the treatment of choice for severe influenza infection but bearing the risk of increased mortality [5]. Whenever a viral disease takes a more severe course, as it is often documented in pandemic situations, the innate immune system, which lives in a fine balance with oral and gut ecosystem and is affected by aging too, is scrambled under an overwhelming overreactive molecular shift pouring great amounts of inflammatory cytokines into the bloodstream [6-8]. The above-mentioned therapeutic strategies uncertainties have left room to tentative herbal remedies interventions.

The concept of such approach is to provide a tentative wider multipronged protective/therapeutic treatment by selective bioactive natural compounds has indeed entered the modern medical field [9-11]. In this respect, traditional Chinese medicine has produced over very long time a multitude of decoctions and capsules [12]. Most of such huge experience has been confined and limited by its empirical aspects and only in the last decade or so, more supporting

scientific researches have been reported [13,14]. Overall, the arena of selected herbal compounds effectiveness is gaining increasing consistency either in experimental as well as in clinical settings, thus calling for a greater attention to natural compounds of potential adjuvant benefit in the treatment of influenza [15,16]. Cordiceps, andrographys and elderberry endowed by a high content of flavonoid anthocyanins, have shown in prior study to exert antiviral and antiinflammatory properties in viral disease, the latter one also very recently reviewed by a metanalysis of randomised controlled studies [17-21]. The aim of the present study was to test the experimental compound GSK/B20 (Viraxil, donated by Named, Italy) which contains the three above herbal extracts added with a blend of antioxidant, vitamin and minerals in some in vitro and in vivo flu models.

Materials and Methods

The herbal complex was prepared according to GMP standards with batch-to-batch consistency. Cell culture. A great care was devoted to start the cultivations with the identical initial conditions. Madin-Darby-Canine-Kidney (MDCK) cells obtained from American Type Culture Collection and cultured in cell culture flasks (Fisher Scientific, USA) with serum-free Dulbecco minimal essential medium MEM (DMEM), supplemented with 10% fetal bovine serum (FBS;

Invitrogen, USA), 1 g/ml of trypsin, 2 mM of l-glutamine, 100 U/ml of penicillin, and 0.1 mg/ml of streptomycin (Sigma-Aldrich, USA). Then, it was incubated at 37°C in a 5% CO₂ atmosphere (cell culture reagents were purchased by Invitrogen, Ontario CA) and humidified incubator. There was no utilization of antibiotics or anti-mycotic agents.

Viruses. All *in vitro* tests were carried out in class II biosafety cabinet. The virus strains used were Influenza A/WSN/33 (H1N1) and Victoria/210/2009 (H3N2) influenza A. All viruses employed in the study were identified and characterised by specific monoclonal antibodies (Respiratory Virus ID kit, Diagnostic Screening Hybrids, Inc., Athens, OH, USA). Aliquots of viral supernatants were five-fold serially diluted with phosphate buffered saline (PBS) pH 7.2.

***In Vitro* Antiviral Test**

Antiviral activity of GPK/B20 was assessed by plaque reduction assay. Before proceeding with viral inoculum, MDCK cells were washed two times with PBS and grown in a medium enriched with DMEM with trypsin TPCK (Merck, Germany), 2 µg/mL of streptomycin/penicillin and 0.3% bovine serum albumin (BSA, Gibco, USA). The virus titer in supernatant was confirmed on MDCK cells using a 50% tissue culture infectious dose (TCID₅₀), as from the method of Reed and Muench [22,23].

Cell co-treatment assay. For the penetration assay, dilutions of GPK/B20 in ice-cold PBS, was incubated in 96-well microtiter plates at the density of 2×10^4 cells/well. The wells were inoculated with a mixture of 100 µL (50% tissue culture infection dose -TCID₅₀-) of virus suspension/well. Then 50 and 100 µg/mL concentrations of GPK/B02 were supplemented with 2 µg/mL TPCK and 0.3% BSA (200 µL/well) at 37°C for 2 h in triplicate. Afterwards the medium was discarded and replaced with new one added with 100 TCID₅₀/well virus for further 2 h. The plates were then incubated in a humidified CO₂ at 37°C so to achieve 90% of viral cytopathogenic effect (CPE) in the control virus. The reaction mixture was assessed for left over viral loaded plaques in MDCK monolayers cells. The medium devoid of GPK/B20 served as control and the amount of antiviral activity was defined by the decrease in the counting of virus plaques. The analyses of the cytopathogenic effect (CPE) were carried out 4–7 days later by reduction assay for antiviral activity. The decrement of viral CPE was assessed by evaluating the colorimetric analysis of cell viability through the tetrazolium salt MTT [3-(4,5-dimethylthiazol-2-yl)-2,5-diphenyltetrazoliumbromide], (Sigma Aldrich, USA). The medium was then collected and 50 µL of DMSO solution was added to the wells. Finally, the plates were washed and dried. Optical density (OD) was determined at 570 nm and the percentage of inhibition was calculated as compared with

that in virus control.

Post-infection CPE Reduction Assay after phytocompound. MDCK cells were seeded into 96-well plates in DMEM, supplemented with 10% FBS and incubated overnight at 37 °C under 5% CO₂. The culture medium was then replaced by the GPK/B20 at two concentrations (medium: 0.2g/kg/day and high: 0.6g/kg/day), separately added to each virus-infected cell culture. This was incubated for 1 hour at 37 °C to enable proper virus adsorption. The unadsorbed virus was inactivated by supplementation with acidic PBS (pH 3) for 1 min, followed with alkaline PBS (pH 11) for neutralization. Plates were monitored for 72h post-infection (hpi) with 12-h time gaps in between and CPE were assessed and scored. The reduction in virus replication was evaluated as a percentage of the virus control (% virus control = CPEexp/CPEvirus control × 100).

Cytotoxicity Assay

GPK/B20 was dissolved in DMSO and diluted to the established concentration with the culture medium when used. The cells harvested from the exponential phase were seeded in 96-well plates in DMEM added with 10% FBS. A culture overnight at 37 °C in 5% CO₂ was started and ALPK/T2Y was then added to the wells to achieve final concentrations ranging from 10⁻⁷ to 10⁻⁵ M incubated at 37 °C in 5% CO₂ for 36 h. Upon completion of the incubation, a stock MTT dye solution (20 µL, 5 mg/mL) was added to each well. After 4h of incubation, 2-propanol (100 µL) was added to solubilize the MTT formazan. The OD of each well was then determined on a plate reader (Tecan Infinite M2000PRO; Tecan Group Ltd., Mannedorf, Swiss). at a wavelength of 570 nm. Viability was calculated using the background-corrected absorbance as follows: Viability (%) = A of experiment well/A of control well × 100%.

Laboratory Animals. The mice were kept in biosafety level 3 polycarbonate individually-ventilated cages and handled in a laminar flow hood cabinet. They were provided with standard laboratory chow food containing 15% (w/w) cocoa butter, 1% (w/w) corn oil and 0.4% (w/w) cholesterol. and water ad libitum. All animal experiments were used in compliance the Institutional Ethical Committee on Laboratory Animal Care and Experimentation. The mice were housed in a specific pathogen-free facility on a 12-hour light/dark cycle and 22–26°C temperature and allowed to acclimatize for 7 days before starting the experiment. Sentinel mice were housed in the same location and regularly checked to confirm the lack of any pathogens.

Experimental mouse flu models. Experiments were carried out on ninety 7- to 10-week-old, 19–23 g male mice which were anaesthetised intraperitoneally with 1%

pentobarbital sodium (0.1 mL/20 g) and randomly divided into 3 groups each. While control mice (group A) were intranasally treated with PBS (group A, n=20), the flu model was established by intranasal infection with 20 mL viral suspension/mouse (viral titer 300 plaque-forming units) of H1N1 virus or H3N2 (group B and C, respectively of 30 mice each). These manouvers were done under isoflurane anesthesia and in a Biosafety Level-2. Twelve hours after H1N1 or H3N2 infection, when prior in-house tests showed a significant morbidity of the animals, (respiratory distress, profound malaise, more than 30% weight loss vs baseline). GPK/B20 supplementation was applied. All groups of mice were daily monitored for two weeks.

Ten mice were randomly selected from each group at 7 days postinfection (dpi) and examined for viral load and lung edema evaluation as detailed below. At the end of experimental study, all living mice of whatever group were euthanased by 0.02 mL/g, ketamine-xylazine.

BAL procedure and differential cells counting. BAL were carried out immediately after mouse euthanasia (at days 10, in each condition),the trachea was exposed and cannulated with a catheter inserted through a small incision under the larynx. Once this was secured with a suture, the lungs were washed three times by instilling 500 μ L of PBS and then gentle aspiration followed. This enabled an 80-90% retrieval of the whole BAL fluid volume flushed. Two repeated BAL were collected from each mouse and pooled on ice before centrifugation (5,000 rpm for 5 min at room temperature). The supernatant was collected and kept at -80°C till measurement of IL-6 and TNF- α levels by using specific high sensitivity kits from RDS (Minneapolis, USA). following the manufacturer's instructions.

Cell pellets were resuspended in 1 ml of RPMI 1640 (Gibco, Carlsbad, CA) added with 2.5% fetal bovine serum (FBS; Gibco,Carlsbad, CA) to count the total cell number by a Thermofisher Scientific cell counter and cytopspins (300 rpm, 3 min, Shandon Cytospin 3 Centrifuge, USA)were prepared at a concentration of 0.3×10^6 cells/ml on SuperFrost glass slides (Thermo Scientific, USA). Cytopspins were air-dried and stained, Thus, the differential cell composition was expressed as percentage of neutrophils, macrophages, and over a total of 400 leukocytes).

Immune cell counting and cytokines assessment in bronchoalveolar lavage fluid. At the end of study period, mice were sacrificed following intraperitoneally injected lethal dose of pentobarbital. Two sequential broncho-alveolar lavages (BAL) were carried out using each time a 0.8 mL of PBS buffer added with 1% BSA. BAL fluid cell from left lobe were counted and differentiated by a Coulter Counter (Beckman Dickson, Fullerton, CA). Samples (200 μ l each)

were centrifuged and then stained with DiffQuick solution (American Scientific, McGraw Park, PA). The right lobe was snap frozen in liquid nitrogen and stored at -80°C to separate RNA to be later homogenized in 250 μ l of DMEM containing 1 μ g/ml of TPCK treated trypsin and 1% BSA for viral titers as described below.

Measurements of IL-6 and TNF- α in BAL fluids. Mouse IL-6 and TNF- α ELISA kits were used (Quantikine immunoassay, R&D, MN), and cytokines in the culture supernatant were assessed followings the manufacturer's instructions. Enzyme immunoassay 96-well plates (Corning Life Sciences, USA) were coated with TNF- α and IL-6 monoclonal antibodies at 4°C overnight. Nonspecific binding sites were blocked with proper buffer for 1h at room temperature and then 100 μ l of a standard was added. BAL fluids were loaded into each well and incubated at 4°C for 24 h. Peroxidase-labeled biotinylated anti-mouse TNF- α and IL-6 monoclonal antibodies were then added and incubated at room temperature for 1 h. The plates were developed using a chromogenic 3,3',5,5'-tetramethylbenzidine substrate (ThermoFisher, USA), and the reaction was stopped with 2N H_2SO_4 . Optical density was measured at 450nm using a Multiskan EX spectrophotometer (Thermo Fisher Scientific, USA).

The lung tissue from each group was divided into three parts, one was used for histopathology examination of immune cells, a second one for cytokine level and tissue gene expression and the third one was centrifuged, and the supernatant used to test the virus titres in the MDCK cells.

Briefly, after 10 days of monitoring, 10 mice from each group were sacrificed. The upper portion of the left lungs was immediately put in 10% neutral buffered formalin and processed for paraffin embedding. Then, ultrathin 5 μ m sections coronal sections were cut and layed on glass slides. (4-mm) were sliced and stained with hematoxylin & eosin or periodic acid Schiff (PAS). by using standard techniques. The further steps complied with the International Harmonization of Nomenclature and Diagnostic Criteria for Lesions in Rats and Mice protocols for respiratory tract disease. Microscopic evaluation was carried out by two distinct pathologists who were unaware of the experimental treatments. Lung histology was photographed by using a calibrated binocular light microscope (Olympus Optical Co.,Tokyo, Japan) set at 100x immersion objective lens and a Zeiss II 10-lines/100 points grid-equipped Zeiss kpl8X (Carl Zeiss Jena GmbH, Jena, Germany). Forty histological fields were counted per section as a default parameter of the study.

Acute pulmonary edema assessment. Lung wet-to-dry (W/D) weight ratio was taken as an index of lung water accumulation during influenza virus infection. Lungs were

removed, quickly weighed to be then dried in an oven at 60°C for 72 h and finally re-weighed as dry weight. Bloodless W/D weight ratio was calculated by measuring hemoglobin concentration of blood (HbB) and lung homogenate supernatant (HbS) and then measuring the lung blood volume (BV) and water volume (WV) by assessing the water fraction in the lung homogenate (WFH), the homogenate supernatant of the (WHS), and the blood fraction (WBF) by $(W_{wet} - W_{dry})/W_{wet}$, where W_{wet} and W_{dry} refer to wet and dry weight, respectively. BV of the lung was calculated by: $BV = 1.039 \times (QH \times WFH \times HbS)/(WHS \times HbB)$ where 1.039 is the blood density and QH is the lung homogenate. WV of the lung was calculated by: $WV = (QH \times WFH) - (BV \times WFB) - W_w$ where W_w is the weight of the water added during homogenization. QW was based on the lung dry weight (lung wet weight - BV - WV) to determine bloodless W/D weight ratios.

Cytokine lung tissue measurements. Lungs were dissected and pulmonary artery cannulated and perfused with PBS to flush any possible intravascular blood out and allow to proceed to whole organ rinsing and drying on a paper tissue. Thereafter, lungs were homogenated using a FastPrep-24 Sample Preparation System (MP Biomedicals, USA) in a Hank's salt solution (1% BSA, 0.1% 0.5M EDTA, protease and RNase inhibitor). The homogenates then subjected to enzyme-linked immunosorbent assay (ELISA). Briefly, mouse ELISA kits for IL-6, and TNF- α were purchased from the DuoSet ELISA kits (R&D, Minneapolis, MN). A microplate reader (Thermo Fisher, USA) set at absorbance wavelength of 450 nm was used to measure cytokine concentration. Uninfected lung samples were also used as an intact control.

Viral Load titer in lung tissue samples. Ten-fold serial dilutions of supernatants of aseptically collected lung homogenates (in EMEM added with 0.1% penicillin-streptomycin) were prepared and inoculated at the amount of 0.1 ml into specific pathogen-free chicken eggs. At 72 hpi, hemagglutination (HA) titers were assayed in allantoic fluids by HA assay. HA titer $\geq 4 \log_2$ were scored as positive. Viral titers were expressed as \log_{10} 50 percent Embryo Infectious Dose or EID50 per ml. One EID50 unit represents the amount

of virus infecting 50 percent of inoculated eggs. The detection limit was a titer of 0.75 \log_{10} EID50/ml, and samples with titers less than 0.75 were equalled to a value of 0.5.

Identification and evaluation of cytokine genes expression in the lung. Western blot lung samples were lysed using RIPA lysis buffer (Beyotime Tech, China). After quantification using a BCA kit (Bio-Rad, USA), a similar quantity of proteins was added to a 10% SDS-PAGE and then moved to polyvinylidene fluoride membranes through a blotting system (Bio-Rad). Skim milk (5% solution) was used to block the membranes and incubated with primary antibodies overnight. Samples were washed three times in Tris-buffered saline added with 0.1% Tween 20, at pH 7.5) and then tested with secondary IL-6- and TNF- α -directed primary antibodies (Cell Signaling Technology, USA). Quantitative RT-PCR. Total RNA (0.5 g) was extracted from ~300 mg of lung tissue following the procedure for the TRIzol Reagent kit from In Vitrogen. The lung tissue was homogenized using a Brinkman Polytron. Chloroform was added, and tubes were spun to separate the phenol and aqueous phase. The aqueous phase was transferred to a new tube, and RNA was precipitated by adding isopropyl alcohol and centrifugation. The RNA pellet was washed in 75% ethanol and redissolved in 15 μ l of diethyl pyrocarbonate-treated water. The amount of RNA was determined spectrophotometrically at 260 nm. One microgram of RNA was immediately reverse transcribed to single-stranded cDNA ReverTraAceqPCR RT Master Mix from Applied Biosystems. Random hexamers were used as primers (table 1). The expression of mRNA was calculated by an Abi Prism 7900HT Sequence Detection System. GAPDH represented the housekeeping reference gene and checked by a specific primary antibody (Santa Cruz Biotechnology, USA). To determine the 18S rRNA and cytokine mRNA levels, a predeveloped primer limited assay from Applied Biosystems was used (Table 1). Each sample was run in triplicate in a volume of 10 μ l for 50 cycles using standard, real-time cycling conditions (ABI 7900 Thermal Cycler system). The cycle threshold values were normalized to a relative standard curve run at the same plate as the samples. The standard curves confirmed an acceptable efficiency, and the ratio of amount of both cytokines mRNA to amount of 18S rRNA was calculated by using the 2- $\Delta\Delta$ CT method.

Genes	Forward (50-30)	Reverse (50-30)
IL-6	CTGCAAGAGACTTCCATCCAG	AGTGGTATAGACAGGTCTGTTGG
TNF α	CAGGCGGTGCCTATGTCTC	CGATCACCCGAAGTTCAGTAG
GAPDH	AGGTCGGTGTGAACGGATTTG	AGGTCGGTGTGAACGGATTTG

Table 1: Primers for cytokine gene expression.

Scanning Electron Microscopy examination. For scanning electron microscopy 6 to 8 lungs blocks per sample were mounted on stubs, sputter coated with gold and examined

using a Jeol 6380 scanning electron microscope. The SEM examination (Phillips SEM 500) was performed first at low magnification (160X) looking for a representative area of the

pulmonary parenchyma while excluding vascular areas. At least 10 images per animal were taken.

Statistics

Statistical analysis was performed using the GraphPad Prism 7.0 software system. The means are geometric means \pm SE. The analysis was performed using Excel 2000 from Microsoft. A repeated-measurement of one-way analysis of variance ANOVA was used to assess the difference along study period. A paired t-test with Bonferroni correction was employed as a post hoc analysis to compare individual time points with the 0-h sample. Systat version 8.0 for Windows (SPSS) was used for this analysis. Significant differences among groups were determined by the Bonferroni Test. p values < 0.05 were considered significant.

Results

Cell co-treatment assay: Cytopathic effect and protection

As compared to control, both viruses used determined a statistically significant cytopathogenic effect on MDCK cells ($p < 0.001$ vs baseline, figure 1). The co-treatment with GPK/B20 brought about a comparably partial protection on monolayer ($p < 0.05$ vs unsupplemented, Figure 1) and in H1NI model, medium dosage was as effective as high dose. However, when analyzing the data in H3N2 model, high dose was yielding a statistically more relevant protective effect unlike in H1Ni ($p < 0.05$). No matter the dosage, however, none of them totally prevented viral cytopathic effect in vitro.

Post-infection CPE Reduction Assay after phytocompound

In the post-infection test of GPK/B20, it appeared that, no matter the flu model, medium dosages mildly but significantly reduced CPE formation ($p < 0.05$ vs control,

Figure 2). However, the reduction achieved by high dosage in H1N1 model proved to be more statistically remarkable than what observed for high dose in H3N2 model ($p < 0.05$ vs medium dosage, Figure 2) were the value was comparable to medium dosage in the same H3N2 model group.

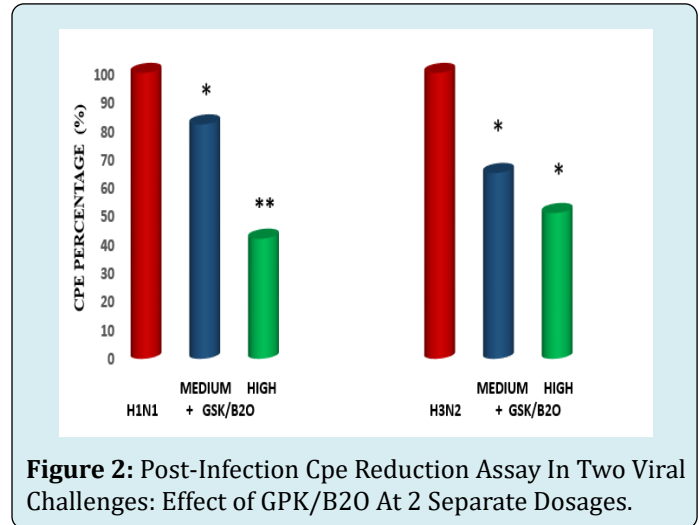


Figure 2: Post-Infection Cpe Reduction Assay In Two Viral Challenges: Effect of GPK/B20 At 2 Separate Dosages.

In vivo data

Measurement of immune cell numbers in bronchoalveolar (BAL) fluid. Both viral models determined a very significant increase of all tested inflammatory cells ($p < 0.001$ vs healthy control, Figure 4). Mice supplemented with GPK/B20 at medium concentration, irrespective of the viral model, did not show any significant improvement of qualitative cellular concentration, although a slight positive trend change appeared. However, medium dosages determined a statistically lower number of recruited macrophages in the viral models and of neutrophils only in H1N1 model ($p < 0.05$ vs untreated control, Figure 4). It also appeared that higher concentration of GPK/B20 determined a statistically significant decrease of inflammatory cells at a higher degree than what obtained by medium dosages ($p < 0.05$, Figure 3).

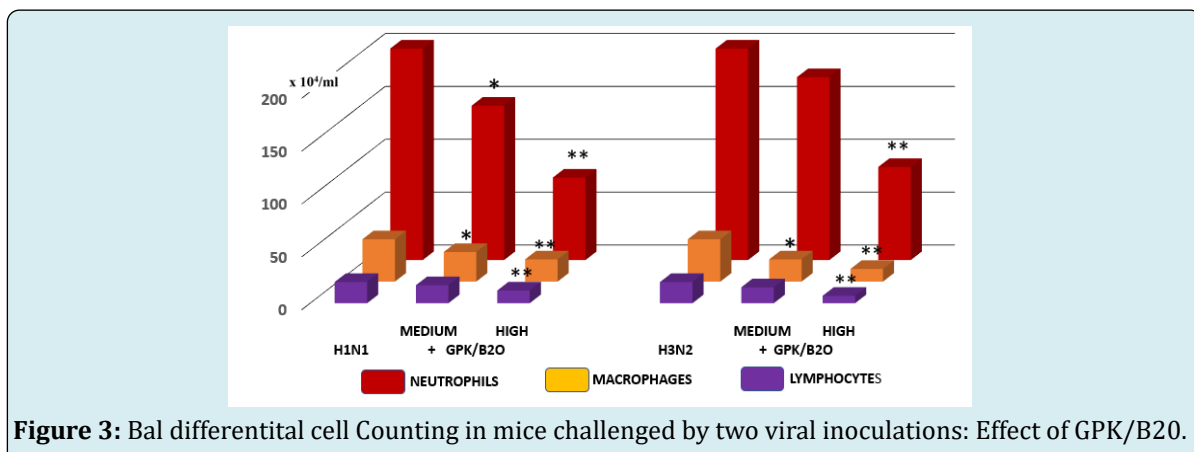


Figure 3: Bal differential cell Counting in mice challenged by two viral inoculations: Effect of GPK/B20.

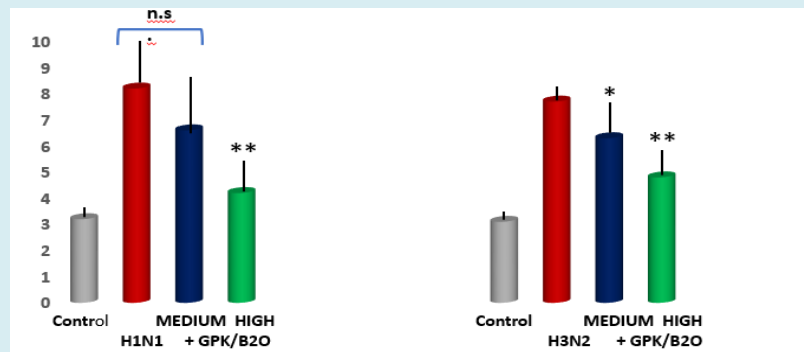


Figure 4: Lung Wet-Dry Weight Ratio In Mice Challenged By Two Viral Inoculations: Effect of GPK/B20.

Acute pulmonary edema assessment. Lung wet/dry weight analysis revealed a significant increase of pulmonary edema in both viral models ($p < 0.001$ vs healthy control, Figure 4). This was partly but significantly mitigated by high dose of GPK/B20 in both viral model ($p < 0.01$ vs untreated models). This data was also significantly better than the ineffective medium dose in H1N1 model ($p < 0.05$ high dose vs medium dosages). Medium dose of GPK/B20 turned to yield a significant improvement in H₃N₂ model ($p < 0.05$ vs untreated group) but at lower efficacy when compared to the high dose ($p < 0.05$, high dose versus medium dose in H3N2 flu model).

Measurements of IL-6 and TNF- α gene expression and concentration in the lung tissue. As compared to control, GPK/B20 at high dose (but not medium dose, data not shown) significantly downregulated the gene expression of the pro-inflammatory genes IL-6 and TNF α ($p < 0.001$ vs control, Figure 5, Figure 6). Similar results were obtaining when testing the BAL level of these cytokines ($p < 0.05$ vs healthy control, Figure 7 and Figure 8), although medium dosage of GPK/B20, also at medium dosage, yielded a statistical decrease of IL-6 (Figure 8).

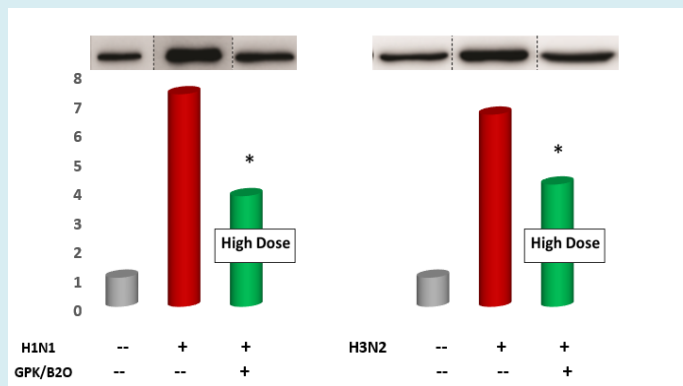


Figure 5: IL-6 Gene Expression in Lung Tissue Level of Mice Challenged by Two Viral Inoculations: Effect of GPK/B20.

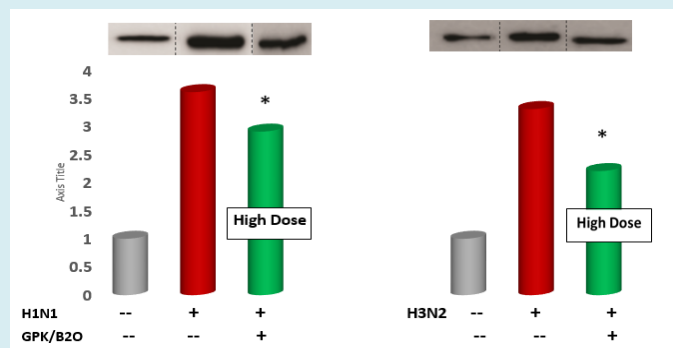


Figure 6: TNF- α Gene Expression in Lung Tissue Level of Mice Challenged by Two Viral Inoculations: Effect of GPK/B20.

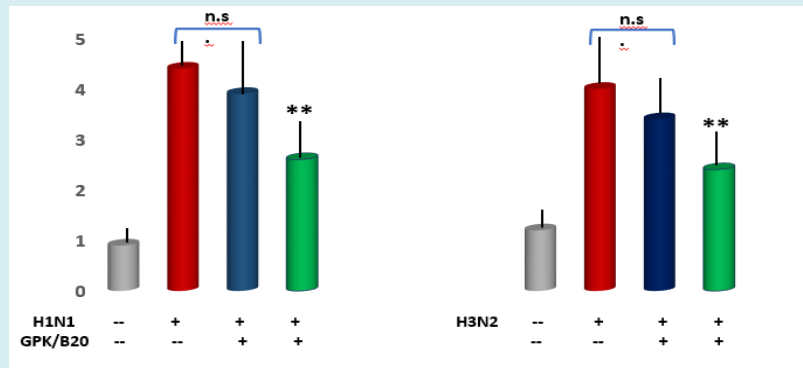


Figure 7: TNF- α Lung Tissue Level in Mice Challenged by Two Viral Inoculations: Effect of GPK/B20.

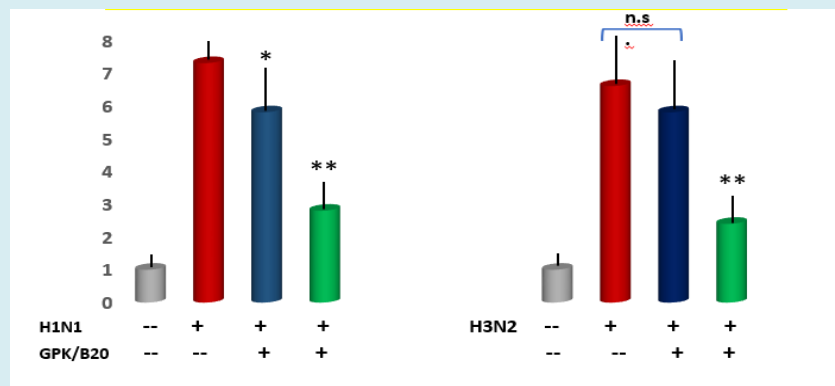


Figure 8: IL-6 Lung Tissue Level in Mice Challenged by Two Viral Inoculations: Effect of GPK/B20.

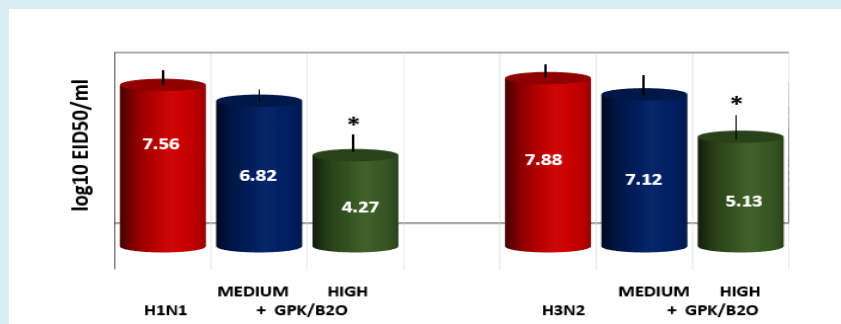


Figure 9: Viral Load in Lung Tissue of Mice Ay 10dpi After Two Viral Inoculations: Effect of GPK/B20.

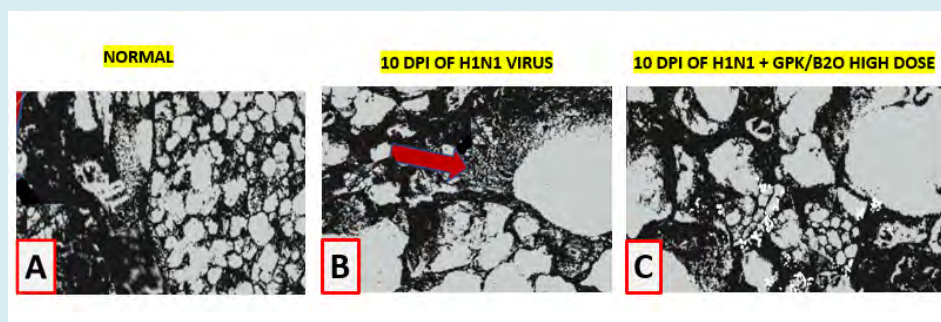


Figure 10: Scanning Electron Microscopy Lung Sections At 10dpi IN H1N1 Challenged Mice: Effect Of GPK/B20.

Lung viral titer as measured by HA. Only high dosages of GPK/B20 showed a statistically decreased viral load, whatever the virus used in the flu model ($p < 0.05$). Whereas medium doses were ineffective).

Scanning Electron Microscopy examination of virus-infected lungs. As compared to control, viral infected lungs showed a profound cellular disarray with plenty of debris and severe inflammatory cells accumulation (red arrow, Figure 10). GPK/B20, when used at high dose, showed to significantly mitigate such features.

Conclusion

A mixture of phytochemicals with some prior scientific support as for their antiviral effect was tested against two different influenza strains, known to be isolated during major seasonal epidemics such as H1N1 and H3N2 [24,25]. The pre-requisite of the present study was to test the in vitro proof of concept that the herewith defined phytochemical would exert meaningful antiviral effect. Data showed that whatever the dosage and the challenged virus employed, GSK/B20 exerted robust antiviral activity either in co-treatment setting and when monitored by post-infection testing. However, more significant results were yielded when using high dose of the phytochemical in H1N1 viral test. These data are in agreement with prior dated findings and more recently re-analysed [26,27]. Although cordiceps has only few data and limited to non-influenza viral disease, we did add it to the phytochemical after a very recent suggestion of its potential benefit and suspect this was of synergistic effect [28]. The same applies to resveratrol whose interest has been very recently revamped during the current pandemic after prior scattered reports [29-31].

The further applicative in vivo study showed that GPK/B20, especially when employed at high dose, significantly limited the lung inflammation in influenza-infected mice bringing about a remarkable drop of the main inflammatory cytokines bursts (IL-6 TNF- α). This phenomenon was paralleled a concomitant downregulation of related genes, when tested at lung tissue level. Epigenetically, this ended up also in a significant decrease of reduction of innate immune cell infiltration (macrophage/monocytes and neutrophils) in mouse lung tissue. This is of course a critical issue, in that while a constant immune surveillance and proper macrophage outburst represent vital elements of defense system, when this is overwhelmed by an acute viral infection, such as in the herewith applied model, the exaggerated chemokine attraction of those cellular population triggers a vicious, self-maintaining circle with deleterious outcome [32]. In such events, as shown very recently in the current pandemic it is well documented how overexpression of IL-6 and TNF- α are associated to heightened morbidity [33,34]. On the other

the administration of GPK/B20 drastically reduced but not abolished the macrophage counting in BAL.

This holds of interest considering that over 10 years ago it had been shown in an experimental setting that the depletion of macrophages and neutrophils resulted in a significant increase in mortality during H1N1 influenza A virus [35,36]. The application of GPK/B20, especially at high dose, proved to significantly prevent the detrimental triad of macro/micro pathological changes associated to cytokine cascade and lung edema, which is the correlate of respiratory distress in humans. In the meantime, more detailed experimental studies are warranted to unveil the range of mechanisms of actions that these natural ingredients are likely to be endowed with [37-39]. In the quest to fight viral attacks, one has also to consider the subtly increasing risk factors associated to aging, obesity and life-style stress, to mention some [40-44]. Although these data have to be taken with caution having been obtained in an experimental-controlled setting and no separate ingredients of the phytochemicals have been tested separately, they suggest a potential safe application in the clinical practice, as recently corroborated [45].

Conflict of interest

All authors declare the absence of any conflict of interest with commercial parties or personal enterprise.

References

1. Kalil AC, Thomas PG (2019) Influenza virus-related critical illness: pathophysiology and epidemiology. *Crit Care* 23(1): 258.
2. Gavigan P, McCullers JA (2019) Influenza: annual seasonal severity. *Curr Opin Pediatr* 31(1): 112-118.
3. Govorkova EA (2013) Consequences of resistance: in vitro fitness, in vivo infectivity, and transmissibility of oseltamivir-resistant influenza A viruses. *Influenza Other Respir Viruses Suppl* 1(1): 50-57.
4. Lampejo T (2020) Influenza and antiviral resistance: An overview. *Eur J Clin Microbiol Infect Dis* 39(7): 1201-1208.
5. Arabi YM, Fowler R, Hayden FG (2020) Critical care management of adults with community-acquired severe respiratory viral infection. *Intensive Care Med* 46(2): 315-328.
6. Jain S, Marotta F, Catanzaro R, Yadav H (2012) Immune system and gut flora interactions are important episodes in metabolic diseases. *J Gastrointest Liver Dis* 21(4):

- 347-348.
7. Illuzzi N, Galli R, Kushugulova A, Zhumadilov Z, Licciardello O, et al. (2014) Expanding the Metchnikoff postulate: oral health is crucial in a successful global aging management strategy. *Rejuvenation Res* 17(2): 172-175.
 8. Nagpal R, Mainali R, Ahmadi S, Wang S, Singh R, et al. (2018) Gut microbiome and aging: Physiological and mechanistic insights. *Nutr Healthy Aging* 4(4): 267-285.
 9. Yadav M, Jain S, Bhardwaj A, Nagpal R, Puniya M, et al. (2009) Biological and medicinal properties of grapes and their bioactive constituents: an update. *J Med Food* 12(3): 473-484.
 10. Jain S, Yadav H, Sinha PR, Marotta F (2009) Modulation of cytokine gene expression in spleen and Peyer's patches by feeding dahi containing probiotic *Lactobacillus casei* in mice. *J Dig Dis* 10(1): 49-54.
 11. Aruoma OI, Hayashi Y, Marotta F, Mantello P, Rachmilewitz E, et al. (2010) Applications and bioefficacy of the functional food supplement fermented papaya preparation. *Toxicology* 278(1): 6-16.
 12. Marotta F, Kumari A, Catanzaro R, Solimene U, Jain S, et al. (2012) A phytochemical approach to experimental metabolic syndrome-associated renal damage and oxidative stress. *Rejuvenation Res* 15(2): 153-156.
 13. Xi S, Li Y, Yue L, Gong Y, Qian L, et al. (2020) Role of Traditional Chinese Medicine in the Management of Viral Pneumonia. *Front Pharmacol* 11: 582322.
 14. Uemura J, Nagpal R, Zerbinati N, Singh B, Marcellino M, et al. (2017) Effect of VBC-1814/7J, a poly-phytocompound, on a non-infectious model of pharyngitis. *Exp Ther Med* 13(6): 3075-3080.
 15. Barak V, Birkenfeld S, Halperin T, Kalickman I (2002) The effect of herbal remedies on the production of human inflammatory and anti-inflammatory cytokines. *Isr Med Assoc J* 4(11): 919-22.
 16. Cervi J, Marotta F, Bater C, Masulair K, Minelli E, et al. (2006) A dietary supplement improves outcome in an experimental influenza model in old mice. *Ann N Y Acad Sci* 1067: 414-419.
 17. Lee HH, Park H, Sung GH, Lee K, Lee T, et al. (2014) Anti-influenza effect of *Cordyceps militaris* through immunomodulation in a DBA/2 mouse model. *J Microbiol* 52(8): 696-701.
 18. Rastananesh R, Marotta F, Tekin I (2020) Call for mobilization of functional foods, antioxidants, and herbal antivirals in support of international campaign to control coronavirus. *Bioactive Compounds in Health and Disease* 3(5).
 19. Ohta Y, Lee JB, Hayashi K, Fujita A, Park DK, et al. (2007) In vivo anti-influenza virus activity of an immunomodulatory acidic polysaccharide isolated from *Cordyceps militaris* grown on germinated soybeans. *J Agric Food Chem* 55(25): 10194-10199.
 20. Yan W, Li T, Zhong Z (2014) Anti-inflammatory effect of a novel food *Cordyceps guangdongensis* on experimental rats with chronic bronchitis induced by tobacco smoking. *Food Funct* 5(10): 2552-2557.
 21. Zakay-Rones Z, Thom E, Wollan T, Wadstein J (2004) Randomized study of the efficacy and safety of oral elderberry extract in the treatment of influenza A and B virus infections. *J Int Med Res* 32(2): 132-40.
 22. Hawkins J, Baker C, Cherry L, Dunne E (2019) Black elderberry (*Sambucus nigra*) supplementation effectively treats upper respiratory symptoms: A meta-analysis of randomized, controlled clinical trials. *Complement Ther Med* 42: 361-365.
 23. Reed LJ, Muench H (1938) A simple method of estimating fifty percent endpoints. *Am J Hyg* 27: 493-4497.
 24. Roychoudhury S, Das A, Sengupta P, Dutta S, Roychoudhury S, et al. (2020) Viral Pandemics of the Last Four Decades: Pathophysiology, Health Impacts and Perspectives. *Int J Environ Res Public Health* 17(24): 9411.
 25. Potter BI, Kondor R, Hadfield J, Huddleston J, Barnes J, et al. (2019) Evolution and rapid spread of a reassortant A(H3N2) virus that predominated the 2017-2018 influenza season. *Virus Evol* 5(2): 046.
 26. Roschek B Jr, Fink RC, McMichael MD, Li D, Alberte RS (2009) Elderberry flavonoids bind to and prevent H1N1 infection in vitro. *Phytochemistry* 70(10): 1255-1261.
 27. Porter RS, Bode RF (2017) A Review of the Antiviral Properties of Black Elder (*Sambucus nigra* L.) Products. *Phytother Res* 31(4): 533-554.
 28. Verma AK, Aggarwal R (2020) Repurposing potential of FDA-approved and investigational drugs for COVID-19 targeting SARS-CoV-2 spike and main protease and validation by machine learning algorithm. *Chem Biol Drug Des*.
 29. Filardo S, Di Pietro M, Mastromarino P, Sessa R (2020) Therapeutic potential of resveratrol against emerging

- respiratory viral infections. *Pharmacol Ther* 214: 107613.
30. Euba B, López-López N, Rodríguez-Arce I, Fernández-Calvet A, Barberán M, et al. (2017) Resveratrol therapeutics combines both antimicrobial and immunomodulatory properties against respiratory infection by nontypeable *Haemophilus influenzae*. *Sci Rep* 7(1): 12860.
 31. Palamara AT, Nencioni L, Aquilano K, De Chiara G, Hernandez L (2005) Inhibition of influenza A virus replication by resveratrol. *J Infect Dis* 191(10): 1719-1729.
 32. Kaiser L, Fritz RS, Straus SE, Gubareva L, Hayden FG (2001) Symptom pathogenesis during acute influenza: interleukin-6 and other cytokine responses. *J Med Virol* 64(3): 262-268.
 33. Malaquias MAS, Gadotti AC, Motta-Junior JDS, Martins APC, Azevedo MLV, et al. (2020) The role of the lectin pathway of the complement system in SARS-CoV-2 lung injury. *Transl Res* S1931-5244(20): 30259-302560.
 34. Kinoshita E, Hayashi K, Katayama H, Hayashi T, Obata A (2012) Anti-influenza virus effects of elderberry juice and its fractions. *Biosci Biotechnol Biochem* 76(9): 1633-1638.
 35. Kim HM, Lee YW, Lee KJ, Kim HS, Cho SW, et al. (2008) Alveolar macrophages are indispensable for controlling influenza viruses in lungs of pigs. *J Virol* 82(9): 4265-74.
 36. Tate MD, Ioannidis LJ, Croker B, Brown LE, Brooks AG, et al. (2011) The role of neutrophils during mild and severe influenza virus infections of mice. *PLoS One* 6(3): e17618.
 37. Krawitz C, Mraheil MA, Stein M, Imirzalioglu C, Domann E, et al. (2011) Inhibitory activity of a standardized elderberry liquid extract against clinically-relevant human respiratory bacterial pathogens and influenza A and B viruses. *BMC Complement Altern Med* 11: 16.
 38. Barak V, Halperin T, Kalickman I (2001) The effect of Sambucol, a black elderberry-based, natural product, on the production of human cytokines: I. Inflammatory cytokines. *Eur Cytokine Netw* 12(2): 290-296.
 39. Fal AM, Conrad F, Schönknecht K, Sievers H, Pawińska A (2016) Antiviral activity of the "Virus Blocking Factor" (VBF) derived i.a. from *Pelargonium* extract and *Sambucus* juice against different human-pathogenic cold viruses in vitro. *Wiad Lek* 69(3): 499-511.
 40. Vaiserman AM, Koliada AK, Marotta F (2017) Gut microbiota: A player in aging and a target for anti-aging intervention. *Ageing Res Rev* 35: 36-45.
 41. Shen X, Miao J, Wan Q, Wang S, Li M, et al. (2018) Possible correlation between gut microbiota and immunity among healthy middle-aged and elderly people in southwest China. *Gut Pathog* 10: 4.
 42. Yadav H, Jain S, Nagpal R, Marotta F (2016) Increased fecal viral content associated with obesity in mice. *World J Diabetes* 7(15): 316-320.
 43. Marotta F, Catanzaro R, Yadav H, Jain S, Tomella C, et al. (2012) Functional foods in genomic medicine: a review of fermented papaya preparation research progress. *Acta Biomed* 83(1): 21-9.
 44. Marotta F, Naito Y, Padriani F, Xuewei X, Jain S, et al. (2011) J Redox balance signalling in occupational stress: modification by nutraceutical intervention. *Biol Regul Homeost Agents* 25(2): 221-9.
 45. Tiralongo E, Wee SS, Lea RA (2016) Elderberry Supplementation Reduces Cold Duration and Symptoms in Air-Travellers: A Randomized, Double-Blind Placebo-Controlled Clinical Trial. *Nutrients* 8(4): 182.

